Critical-point rheology of a sheared phase-separating micellar solution

K. Hamano, T. Ishii, and M. Ozawa
Department of Biological and Chemical Engineering, Faculty of Technology, Gunma University, Kiryu, Japan

J. V. Sengers
Department of Chemical Engineering and Institute for Physical Science and Technology, University of Maryland, College Park, Maryland 20742

A. H. Krall
Exxon Research and Engineering Company, Annandale, New Jersey 08801

(Received 3 May 1994)

We have investigated the rheological behavior of a phase-separating critical mixture of a nonionic micellar solution with a lower consolute point. For this purpose we have observed forward light scattering and measured the viscosity during the phase-separation process that occurs after quenches into the unstable region. The light-scattering experiments show that at a finite shear rate S the formation of concentration domains is suppressed until a characteristic temperature T_S larger than the critical temperature T_c is reached. After quenches to temperatures $T > T_S$, concentration domains strongly elongated in the direction of the flow are formed. We observe an effective viscosity enhancement $\Delta\eta(t)$ as a function of the time t after the quench which depends on the shear rate S and which decays to zero as $t \to \infty$. The approach to a nearly stationary state after quenching, where $\Delta\eta \simeq 0$, is accompanied with the formation of a stringlike morphology of concentration domains which does not resist shearing in contrast to recent theoretical predictions which assume that the decay of the viscosity enhancement is due to coalescence of the domains.

PACS number(s): 05.70.Jk, 47.55.Kf, 83.70.Hq

I. INTRODUCTION

In a critical liquid mixture, brought into an unstable state inside the coexistence boundary, spinodal decomposition can occur [1,2] and a randomly interconnected or percolated morphology of concentration domains can be formed [3]. When shear is applied to such phase-separating mixtures in a macroscopic flow field, viscous stresses may be responsible for the deformation and breakup of these domains, resulting in an irreversible transformation of mechanical energy into thermal energy. This dissipation mechanism may lead to an enhancement of the observed macroscopic viscosity. While intuitively plausible, this effect was predicted only recently [4–6], leading to some attempts to investigate the phenomenon experimentally [7,8]. Because of the principle of critical-point universality [2,9], we suggest that phase-separating mixtures near a critical mixing point are interesting candidates for studying these types of rheological effects, sometimes referred to as critical-point rheology [5].

Domain morphology under shear was observed by van Dijk, Eleveld, and van Veelen in a rubber blend by applying a technique of phase-contrast optical microscopy [10]. Their observations suggest the presence of considerably stretched domains with a strong anisotropy ratio $R_{\parallel}/R_{\perp}$ of about 10 under steady shear flow, but stretched domains are also suggested by recent light-scattering experiments [11-13] and also by computer simulations [6,14,15]. Clear evidence of the formation of long tubelike structures of concentration domains in a sheared polymer mixture has been reported most recently by Hashimoto *et al.* from experimental observations with a microscope [16]. This rheological behavior of critical phase-separating mixtures appears to differ in a significant way from that expected on the basis of current theory [5,17].

The research reported in the present paper is concerned with the rheological behavior of a critical phase-separating mixture. Specifically, we have examined the behavior of a critical phase-separating nonionic micellar solution subjected to flow between two rotating concentric cylinders. The experiments have been performed with a nonionic micellar solution of tetraethylene glycol *n*-decylether ($C_{10}E_4$) and water, which is a portion of the sample employed in our previous work [18-22]. A micellar solution, consisting of a nonionic surfactant and water, can create self-assembling spherical microstructures (micelles) with typical sizes of a few nm in water. The mixture $C_{10}E_4 + H_2O$ has a lower consolute point, so that phase separation occurs upon raising the temperature [23]. It has been demonstrated that the asymptotic critical behavior of this micellar solution is identical to that observed in ordinary liquid mixtures with a critical mixing point, and the micellar solution belongs to the same static and dynamic universality class of critical phase transitions [18–23]. Because of this universality of critical behavior, we expect that the experimentally observed

shear effects near the critical point of $C_{10}E_4+H_2O$ will also be applicable to other critical liquid mixtures. In view of the limited studies thus far reported for the rheological behavior of micellar solutions, the present research will contribute to a better understanding of how such systems behave under flow [24].

II. EXPERIMENT

The experiments were performed with a rotational viscometer of the Zimm-Crothers type [25]. In addition, a provision was made enabling us to observe simultaneously light scattered by the micellar solution. A schematic representation of the viscometer is shown in Fig. 1. The rotational viscometer consists of an inner and an outer cylinder, both made of Pyrex. The inner cylinder is about 8 cm long, and has an outer diameter of 10.00 ± 0.02 mm. The surrounding outer cylinder has an internal diameter of 12.05 ± 0.04 mm, leaving a gap of 1.03 ± 0.04 mm between the two cylinders. The portion of the solution between the two cylinders is subjected to shear by driving the inner cylinder with an electrically induced magnetic field whose strength is varied continuously. For this purpose a cylindrical piece of aluminum with a height of 25 mm and with an inner diameter of 5 mm is mounted inside the inner cylinder, as indicated in Fig. 1. Two pairs of magnetic coils (MC's) are located on a horizontal plate outside the viscometer as indicated in Fig. 2, which shows a top view of the experimental arrangement. In adapting this method to rotational viscometry, we were inspired by previous work of Einaga, Miyaki, and Fujita [26]. The weight of the aluminum piece inside the inner cylinder was adjusted so as to guarantee that the

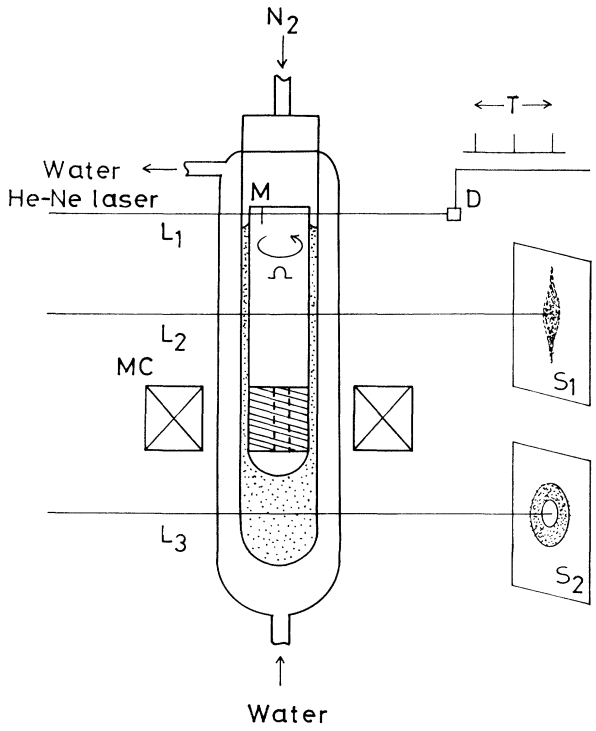

FIG. 1. Schematic representation of the rotational viscometer and of the level of the laser beams.

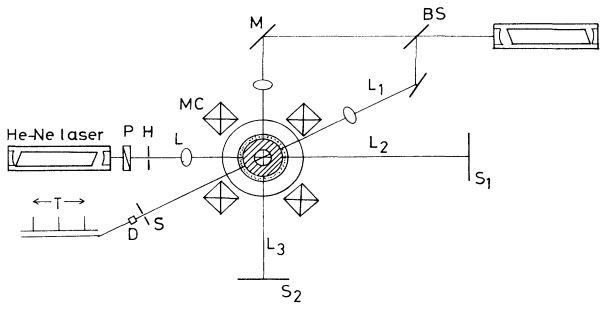

FIG. 2. Top view of the experimental arrangement.

inner cylinder would float in the solution, leaving the solution below the bottom of the inner cylinder effectively unaffected by the shear. Moreover, prior to the measurements careful precautions were made to ensure that this inner cylinder would float in the vertical position. Water from a temperature-regulated bath flows through a jacket surrounding the outer cylinder, thus maintaining the viscometer at a constant temperature.

The liquid in the gap between the two cylinders is subjected to a shear rate which is calculated from the imposed angular velocity of the inner cylinder and the inner and outer cylinder diameters. The viscometer was calibrated with water as the calibrating liquid [27]. The viscosity η and the shear rate S were determined with an absolute accuracy of 3% and 2%, respectively.

Three laser beams originating from two He-Ne lasers as indicated in Fig. 2 are allowed to pass through the cylinders of the viscometer. Laser beam L_1 passes at a level above the surface of the liquid solution and serves to measure the angular velocity of the inner cylinder with the aid of a mark M as indicated in Fig. 1. Laser beam L_2 passes through the cylinders diametrically at a height corresponding to the middle of the inner cylinder, and is used to observe the light scattered in the forward direction by the sheared mixture. To observe simultaneously the light scattered by a nearly quiescent mixture, another laser beam L_3 passes through the bulk mixture in the viscometer at a level about 1 cm below the bottom of the inner cylinder.

The same apparatus was used for some of our previous experiments [13,18,21]. For the present experiments allowance was made to vary the pressure P so as to induce spinodal decomposition by applying pressure quenches [28,29]. The pressure was supplied to the mixture in the viscometer with dry nitrogen. For this purpose a pressure line, consisting of teflon and stainless steel tubing with a three-way cock and three magnetic switches, was connected to the top of the rotational viscometer [30]. Prior to the quench experiments we measured the critical temperature T_c as a function of the pressure P over the range $0.13\leq\Delta P\leq1.94$ bar, where $\Delta P=P-P_0$, with P_0 being the atmospheric pressure. From a fit to these data we found

$$\frac{dT_c}{dP}=10.7\pm0.4\ \text{mK/bar}\ . \tag{2.1}$$

Since dt_c/dP is positive, and since our micellar solution

has a lower critical mixing temperature, we can induce spinodal decomposition by starting from a state with elevated pressure $P=P_0+\Delta P$ at a fixed temperature T near but slightly below $T_c(P)$ and then suddenly decreasing the pressure to $P=P_0$ at the same temperature. In principle a sudden adiabatic pressure change could also affect the temperature T [31,32], but this effect appears to be negligible in our system. This procedure is equivalent to quenching the temperature relative to the critical temperature from an initial small negative value $T-T_c(P)$ to a final positive value $T-T_c$, where we indicate the critical temperature at atmospheric pressure $P=P_0$ by T_c. Even though spinodal decomposition is induced by a pressure quench, we shall refer to the corresponding final value $\Delta T=T-T_c$ as the quench depth. In practice we performed these quenches at nonzero values of the shear rate S. While the critical temperature T_c is also expected to depend upon the shear rate S [33,34], this effect is estimated to be at most a few mK in our experimental shear-rate range, so that $T-T_c(S)\simeq T-T_c$.

All experimental results reported in the present paper have been obtained with the concentration of $C_{10}E_4+H_2O$ being at the critical concentration [18], and at temperatures near the critical temperature T_c.

III. SUMMARY OF PREVIOUS RESULTS

In order to elucidate the approach adopted in the experiments to be reported here, we first summarize some results previously obtained for $C_{10}E_4+H_2O$ near the critical point [18-22]. This micellar solution belongs to the same static and dynamic universality class as ordinary liquid mixtures with a critical point of mixing. Specifically, the correlation length ξ of the critical fluctuations diverges at the critical concentration as

$$\xi=\xi_0\varepsilon^{-\nu}\ , \tag{3.1}$$

where $\varepsilon=|T-T_c|/T_c$. The critical exponent $\nu=0.630$ is universal, and the system-dependent amplitude ξ_0 has the value $\xi_0=(10.7\pm0.5)\times10^{-8}$ cm for $C_{10}E_4+H_2O$ [19]. The lifetime τ_ξ of the critical fluctuations is given by [35]

$$\tau_\xi=6\pi\eta\xi^3/k_BT\ , \tag{3.2}$$

where k_B is Boltzmann's constant. In evaluating shear-induced effects near the critical point, one distinguishes between a weak-shear regime corresponding to $S\tau_\xi<1$ and a strong-shear regime corresponding to $S\tau_\xi>1$ [5]. In the absence of shear or, equivalently, for $S\tau_\xi\ll1$, the viscosity η diverges as [18]

$$\eta\propto\xi^x\ , \tag{3.3}$$

where $x\simeq0.065\pm0.008$, in good agreement with the universal value observed for ordinary liquid mixtures [7,36,37]. On the other hand, at $T=T_c$ the viscosity depends on the shear rate S such that [22]

$$\eta\propto(S)^{-\omega}, \tag{3.4}$$

with $\omega=0.021\pm0.003$ in excellent agreement with the theoretical prediction [38] $\omega=x/(3+x)$.

The results quoted above pertain to the micellar solution near the critical point in the homogeneous one-phase region. In the present experiments we have brought the system into the unstable region above the critical temperature. The correlation length of the critical fluctuations in the coexisting phases above the critical temperature is given by

$$\xi'=\xi_0'\varepsilon^{-\nu}\ , \tag{3.5}$$

with $\xi_0'/\xi_0=0.51$ [39], so that $\xi_0'=5.45\times10^{-8}$ cm. The lifetime $\tau_{\xi'}$ of the critical fluctuations inside the phase boundary is in analogy to (3.2),

$$\tau_{\xi'}=6\pi\eta(\xi')^3/k_BT\ , \tag{3.6}$$

while the weak- and strong-shear regimes now correspond to $S\tau_{\xi'}<1$ and $S\tau_{\xi'}>1$, respectively. For $S\tau_{\xi'}\ll1$ the viscosity again diverges in accordance with (3.3), so that

$$\eta\propto(\xi')^x\ . \tag{3.7}$$

To study the effect of shear on the phase-separating process near the critical point, we entered the region inside the phase boundary by raising the temperature T to a value above T_c for finite values of the shear rate S in some previous experiments [22]. Somewhat to our surprise, we found from observing the light-scattering patterns at a fixed value of the shear rate S that the system remained in a nearly spatially homogeneous state even at temperatures above $T_c\simeq T_c(S)$, until a characteristic temperature $T_S(S)$ was reached where a sharp and intense streak perpendicular to the direction of shearing appeared. This characteristic temperature $T_S(S)$ appeared to vary with the shear rate S as [22]

$$|T_S-T_c|/T_c=\varepsilon_0S^p\ , \tag{3.8}$$

where $p=0.51\pm0.03$ and $\varepsilon_0=(1.35\pm0.11)\times10^{-5}$, with S specified in s^{-1}.

We subsequently studied this phenomenon in more detail in an isobutyric acid plus water mixture near the critical point [13]. Even though the exponent p in the power law (3.8) agrees with the value $p=1/\nu(3+x)$ predicted theoretically for the variation of the critical temperature T_c with the shear rate S [33], it was determined that the observed characteristic temperature $T_S(S)$ should not be identified with $T_c(S)$ but with the temperature where $S\tau_{\xi'}\simeq1$, i.e., where the crossover between the strong- and weak-shear regimes occurs [13]. The rheological phenomena associated with the strong- and weak-shear regimes in the region inside the phase boundary differ from those in the strong- and weak-shear regimes in the one-phase region outside the phase boundary. For $S\tau_{\xi'}<1$, i.e., for $T_c<T_S(S)<T$, a shear rate has a negligible effect on the lifetime of the fluctuations, while concentration domains are present which are deformed significantly by the shear. Thus in the strong-shear regime no concentration domains have been observed, while in the weak-shear regime strongly anisotropic concentration domains appear, as we shall further demonstrate in Sec. IV.

IV. EXPERIMENTAL RESULTS

A. Light scattering during phase separation

To study the effect of shear on the phase-separation process near the critical point, we entered in the present experiments thermodynamic states inside the phase boundary through fast pressure quenches by dropping the pressure P from an initial elevated value $P_0+\Delta P$ to atmospheric pressure P_0, as explained in Sec. II, at a given fixed value of the shear rate S. To specify the nature of the shear-affected state immediately after the pressure quench, we introduce a dimensionless variable

$$\delta_S=(T_S-T_c)/(T-T_c)\ , \tag{4.1}$$

where T_S is the shear-rate dependent characteristic temperature as given by Eq. (3.8) and where T is the temperature at which the pressure quench is applied. Thus $\delta_S<1$ corresponds to the weak-shear regime, and $\delta_S>1$ corresponds to the strong-shear regime as defined in Sec. III.

In a first set of experiments, immediately after applying a pressure quench so as to insure that $T>T_c$, we applied a "shear quench" [40,41] by suddenly dropping the shear rate S to zero by stopping the rotation of the inner cylinder of the rotational viscometer. We registered the forward-scattered light on a video camera, and on a photographic film after the shear quench.

In Fig. 3 we show three pairs of photographs of forward-scattered light from the phase-separating critical mixture at a fixed temperature $L\simeq T_c+18$ mK after cessation of the shear from initial states of shearing with three different shear rates S. The photographs designated with capital letters show forward-scattering patterns in the very early stage after cessation of the shear, and the photographs designated with lower-case letters were obtained at substantially later times. The three experiments correspond to $\delta_S\simeq 0.20$ [(A) and (a)], $\delta_S\simeq 0.63$ [(B) and (b)], and $\delta_S\simeq 1.47$ [(C) and (c)]. Thus photographs (A) and (a) probe the weak-shear regime $S\tau_{\xi'}<1$, photographs (C) and (c) probe the strong-shear regime $S\tau_{\xi'}>1$, while photographs (B) and (b) correspond to a near-crossover case with $S\tau_{\xi'}$ smaller than but close to unity. In the initial stage after cessation of the shear, we observe strongly anisotropic scatterings of light perpendicular to the flow direction in photographs (A) and (B) corresponding to $S\tau_{\xi'}\leq 1$, while the effect is very weak in photograph (C). According to our present understanding, as elucidated in Sec. III, highly anisotropic concentration domains are present in the weak-shear regime $\delta_S<1$. The intense anisotropic forward scattering in photographs (A) and (B) confirms the presence of concentration domains elongated along the flow direction for $\delta_S\leq 1$, and is consistent with recent observations in sheared polymer mixtures [16]. On the other hand, the formation of such stringlike concentration domains ordered in space along the flow direction is suppressed in the strong-shear regime $\delta_S>1$.

Photographs (a), (b), and (c) show three characteristic light-scattering patterns in the late stage after cessation of the shear. Photograph (c), which corresponds to the strong-shear regime with $\delta_S=1.47$, shows the appearance of nearly isotropic scattering with a characteristic wavelength. That is, we observe a spinodal ring similar to those observed as a result of spinodal decomposition when a critical mixture is quenched into the unstable region by a temperature or a pressure quench without shear [1]. The wavelength associated with the observed spinodal ring corresponds very well to the characteristic length of the growing domains, whose growth was initially suppressed by the shear [22]. On the other hand, in the weak-shear regime with $\delta_S\cong 0.20$, we observe a slow relaxation of the pattern of scattered light from photograph (A) to photograph (a). Thus in contrast to the strong-

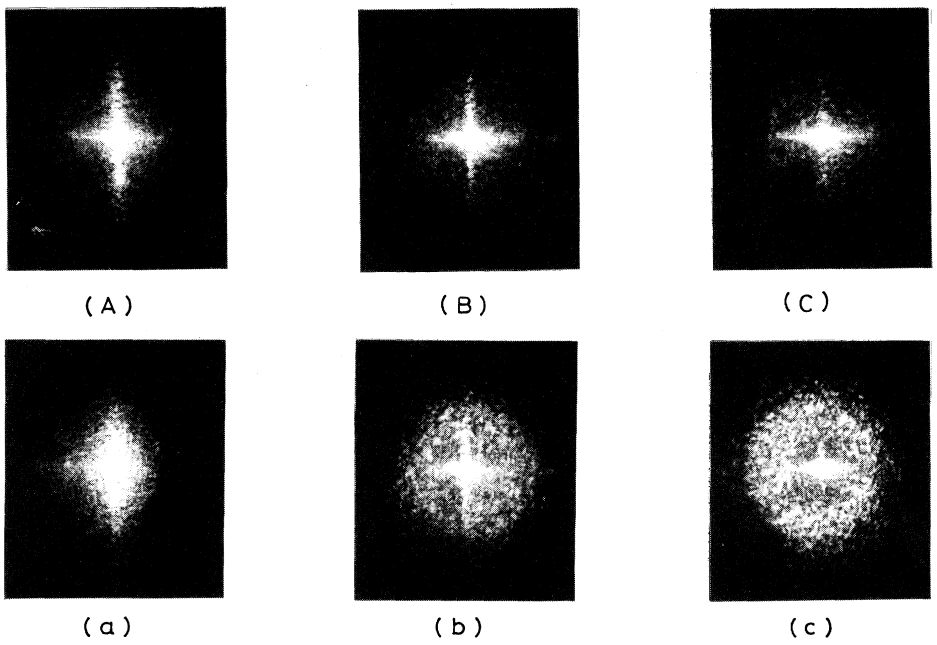

FIG. 3. Patterns of light scattered in the forward direction from the phase-separating critical mixture at $T\simeq T_c+18$ mK after cessation of the shear from $S\simeq 0.8$ s^{-1} to 0 [(A) at $t\simeq 3$ s and (a) at $t\simeq 55$ s], from $S\simeq 7.6$ s^{-1} to 0 [(B) at $t\simeq 10$ s and (b) at $t\simeq 36$ s], and from $S\simeq 42$ s^{-1} to 0 [(C) at $t\simeq 3$ s and (c) at $t\simeq 35$ s].

shear case, we now do not observe any characteristic wavelength associated with growing concentration domains. Particularly interesting is the simultaneous observation in photograph (b) of both a weakly anisotropic spinodal ring and a persistent sharp streak of intense forward scattering in the direction of the flow. A similar observation has also been reported recently by Beysens, Perrot, and Baumberger [42].

We conclude that the observations shown in Fig. 3 indicate the presence of two mechanisms of phase separation after a shear quench. In the strong-shear regime the mixture remains homogeneous even though $T > T_c$, and after cessation of the strong shear ($\delta_S > 1$) the phase separation is similar to the spinodal decomposition observed in critical mixtures without shear. In the weak-shear regime $\delta_S < 1$ highly anisotropic concentration domains in the form of long tubes oriented parallel to the flow are present [16]. In the absence of shear the development of such anisotropic domains would be prevented by a capillary instability associated with the interfaces of these concentration domains, which amplifies gradients of the local interfacial structure [43]. Apparently the shear suppresses the capillary instability, so that long tubes with relatively constant diameter can be formed. The spatial orientation of the domains might also have a stabilizing effect, as suggested by Hashimoto *et al.* [16]. To explain the appearance of an only weakly anisotropic spinodal ring in photograph (b) corresponding to $\delta_S \cong 0.63$, we conjecture that some of the long tubelike concentration domains may rapidly lose their spatial orientation or elongated shape after cessation of the shear, whereupon the capillary-driven instability might precipitate the rapid coalescence much like in the process of spinodal decomposition in a quiescent mixture. Though speculative and *ad hoc,* our argument is physically appealing and in accordance with our observations.

B. Viscosity during phase separation

To investigate the effects of the stringlike domains induced by the shear on the viscosity of the phase-separating mixture, we performed a second set of experiments in which the viscosity η was measured as a function of time after the system was brought into the unstable region by a pressure quench but maintaining the shear rate S at a nearly constant value throughout the entire process. These experiments were not done at a fixed (positive) value of T-T_c, but at a fixed (positive) value of T-T_S, where the notation T_S continues to refer to the shear-rate dependent characteristic temperature at atmospheric pressure as given by Eq. (3.8). For this purpose we first raised the temperature at a given shear rate S and at a given elevated pressure $P = P_0 + \Delta P$ to a value $T = T_S(P)$ following the same procedure as in previous experiments [22], and assuming that dT_S/dP is equal to dT_c/dP. We then applied a pressure quench by dropping the pressure from $P_0 + \Delta P$ to P_0. In practice we used $\Delta P = 1.96$ bar, resulting in $T - T_S \simeq 21$ mK. Hence, all these experiments correspond to the weak-shear regime but with different values of the shear rate S.

In Fig. 4 we show the viscosity measured as a function of the time t after the pressure quench obtained at three different shear rates, namely $S \simeq 0.2$, 0.75, and 38 s^{-1}. We have actually plotted the ratio η/η_S, where η_S is the viscosity measured just prior to the pressure quench, when $T = T_S(P)$, so that $T - T_c \simeq T_S - T_c$, i.e., $\delta_S \simeq 1$. We observe a rapid enhancement in η/η_S followed by a slow decrease as a function of time. This feature appears to be similar to our earlier observations for a spinodally decomposed critical mixture of simple liquids, when we studied the phenomenon in an oscillatory shear field as a function of the quench depth [7,44,45]. The present experimental arrangement allows us to investigate the phenomenon as a function of a steady shear rate S. As is evident from Fig. 4, we observe a significant enhancement in η/η_S at the lower rates of shearing, while little or no enhancement is encountered at the high shear rate $S = 38$ s^{-1}.

Our experimental results suggest that the system tends to approach a certain stationary state in which η/η_S has decreased to a value somewhat smaller than unity. Moreover, this stationary state is reached faster the higher the shear rate S. To investigate this tendency, we postulate that this stationary state corresponds to $\eta = \eta^*$, where η^* is to be identified with the viscosity η of the two coexisting phases. From Eqs. (3.5) and (3.7) it follows that we may estimate η^*/η_S as $\eta^*/\eta_S = \delta_S^{yx}$, since η_S corresponds to $\delta_S \simeq 1$. Values for η^*/η_S thus obtained are

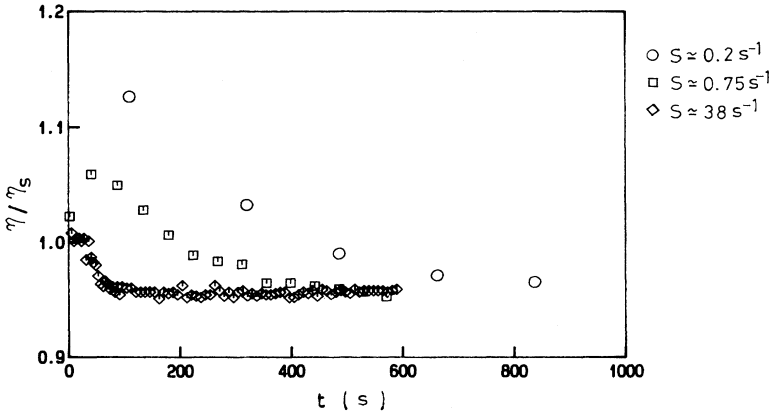

FIG. 4. Viscosity ratio η/η_S of the phase-separating critical mixture as a function of the time t following quenches to $T \simeq T_S + 21$ mK. Here η_S is the viscosity observed at $T \simeq T_S(P)$ just prior to the pressure quench to P_0.

0.90, 0.93, and 0.97 for $S=0.2$, 0.75, and 38 s^{-1}, respectively, approximately compatible with the limiting values approached in Fig. 4. Hence we define the critical viscosity enhancement as $\Delta\eta=\eta-\eta^*$; this enhancement is a function of both the shear rate S and the time t. In Fig. 5 we have plotted the ratio $\Delta\eta/\eta^*$ as a function of the logarithm of the product St; the dashed line indicates a slope of -0.06. We note that the decrease of $\Delta\eta/\eta^*$ with increasing St, observed at different shear rates S, is roughly similar, and the values do decay to a limiting value of $\Delta\eta/\eta^*\simeq 0$. It may therefore be concluded that a stationary state is reached for large values of St. The approximate scaling with the product St implies that this stationary state is reached faster as the shear rate becomes larger.

An understanding of the physical phenomenon causing this behavior is of considerable interest. Just prior to the pressure quench the crossover temperature $T_S(P)$ is just above the actual temperature T, and, as we have seen, no concentration domains are present at temperatures between $T_c(P)$ and $T_S(P)$. However, after the pressure quench T_S is 21 mK below the actual experimental temperature T, and in this regime anisotropic concentration domains are formed as a result of the imposed shear. The sharp spikes in the light-scattering pattern indicate that at higher shear rates S these domains become extremely elongated. On the other hand, we observe that at the higher shear rates $\Delta\eta/\eta^*$ approaches zero much more rapidly. We therefore conclude that the decrease of $\Delta\eta/\eta^*$ to zero is associated with the degree of stringiness of the concentration domains formed under shear, and not associated with the coalescence of domains during spinodal decomposition as suggested in the literature [4,17]. Our data show that $\Delta\eta/\eta^*$ roughly decays as

$$\Delta\eta/\eta^*\sim-\kappa^{-1}\ln(St)\ , \tag{4.2}$$

with $\kappa^{-1}\simeq 0.06$. On the other hand, Onuki [5] estimated the effective viscosity enhancement to be of the order of η^*, since the capillary pressure σ/R and the shear stress η^*S must balance in each characteristic domain in the case that the Reynolds number is sufficiently small. He considered that a surface energy σR^2 associated with the domain must be supplied during deformation till the eventual breaking up in a time scale of the order of S^{-1}, giving rise to the dissipation of this surface energy into heat. This mechanism implies $\Delta\eta/\eta^*$ to be of order unity. Onuki also assumed that the breaking up of the domain occurs with $R_\parallel\sim R_\perp$. This condition may be satisfied when the domain feels the shear very weakly, and we infer that this could occur in the case of small shear rate $S\simeq 0.2$ s^{-1} in our experimental range. We find roughly $\Delta\eta/\eta^*\simeq 0.4$ for $St=1$ when $S=0.2$ s^{-1}, which is compatible with the order of magnitude of Onuki's estimate. In this case it follows from Eq. (4.2) that the steady state with $\Delta\eta/\eta^*=0$ will only be reached after a very long relaxation time $t_S\simeq S^{-1}\exp(0.4\kappa)$, which is about 4000 s for $S\simeq 0.2$ s^{-1}. With regard to this point, Ohta, Nozaki, and Doi [6] have commented upon an interesting behavior shown by their computer simulations of critical phase separation under very weak shear. They considered an interface tensor with elements [6]

$$q_{\alpha\beta}=V^{-1}\int d\Omega(n_\alpha n_\beta-\tfrac{1}{3}\delta_{\alpha\beta})\ , \tag{4.3}$$

where n_α and n_β are components of the unit vector normal to the surface element $d\Omega$ of the interface, where $\delta_{\alpha\beta}$ is the Kronecker delta, and where the integral is taken over all interfaces in the volume V. The interface tensor vanishes when the interfaces on average are isotropically oriented. However, in the computer simulations they found that the interface tensor associated with the domains in the presence of shear did not reach a steady state value even at very large St, and that long domains lying along the flow direction were formed, which phenomenon is consistent with our experimental results.

In a subsequent paper [17], Doi and Ohta (DO) developed a set of phenomenological constitutive equations for a mixture of two immiscible fluids subjected to shear flow. The DO equations include two quantities characterizing the system, namely the viscosity η^* and the interfacial tension σ. We identify η^* with the experimental η^*, which we further assume to be equal to the viscosity free from the contribution of domains. It is worthwhile to compare our results with the DO theory, although Doi and Ohta did not anticipate the formation of stringlike phases at increasing shear rates. For our case the DO equations become

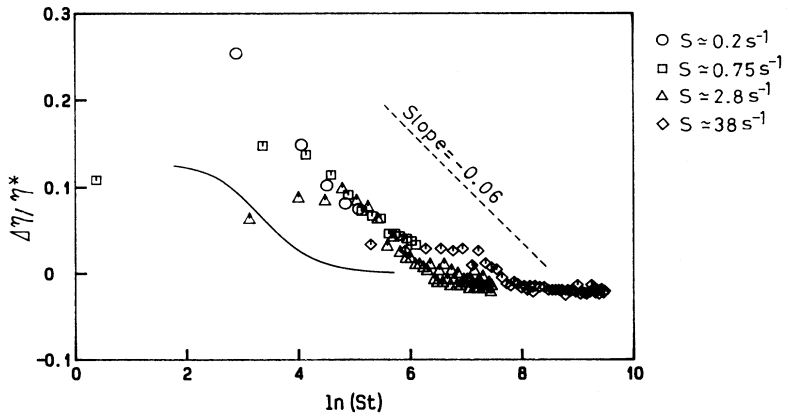

FIG. 5. The reduced viscosity enhancement $\Delta\eta/\eta^*$ as a function of $\ln(St)$, where η^* is the viscosity expected for the two coexisting equilibrium phases. The dashed line indicates a slope -0.06. The solid curve represents values calculated from the theory of Doi and Ohta with $\mu=1$.

$$\frac{\partial q_{xy}}{\partial t}=S\left[\frac{q_{xy}^2}{Q}-q_{xx}-\frac{Q}{3}\right]-\frac{c_1}{\mu}\frac{\sigma}{\eta^*}Qq_{xy}\ , \tag{4.4}$$

$$\frac{\partial q_{xx}}{\partial t}=S\left[\frac{q_{xy}q_{xx}}{Q}+\tfrac{2}{3}q_{xy}\right]-\frac{c_1}{\mu}\frac{\sigma}{\eta^*}Qq_{xx}\ , \tag{4.5}$$

$$\frac{\partial Q}{\partial t}=-Sq_{xy}-c_1\frac{\sigma}{\eta^*}Q^2\ , \tag{4.6}$$

where Q is the interfacial area per unit volume, and where $c_1>0$ and $0\le\mu\le 1$ are two phenomenological parameters related to the relaxation rates of the interfacial area and the interfacial anisotropy. The first term on the right-hand side of each of the equations (4.4)–(4.6) represents free streaming of the interface in the flow, and the second term its decay in the absence of flow. The shear-stress component Γ_{xy} is given by $\Gamma_{xy}=\eta^*S-\sigma q_{xy}$ and $\Delta\eta=\Gamma_{xy}/S-\eta^*$, so that $\Delta\eta/\eta^*=-(\sigma/\eta^*S)q_{xy}$. For the stationary state $t\to\infty$ with $\partial q_{xy}/\partial t=\partial q_{xx}/\partial t=\partial Q/\partial t=0$, this result implies

$$\lim_{t\to\infty}\frac{\Delta\eta}{\eta^*}=\frac{\mu(1-\mu)}{3c_1(1+\mu)^2}\ . \tag{4.7}$$

From Eq. (4.7) it follows that in order to reach a steady state with $\Delta\eta/\eta^*\simeq 0$ the parameter μ must be unity, since $\mu=0$ is unphysical. As a limiting case we shall use the value $\mu=1$. This means that we neglect the term associated with the relaxation of interfacial anisotropy. In this case the decay of the interfacial anisotropy tensor q_{xy} is due entirely to the decay of Q, the extent of the interface itself. Therefore, within DO theory, the behavior $\Delta\eta/\eta^*\to 0$ requires $Q\to 0$ also. To compare our result with the DO theory, we need to evaluate c_1 and assign an initial value Q_0 to Q. Since Eq. (4.6) yields $Q^{-1}=c_1(\sigma/\eta^*)t+Q_0^{-1}$ for the case of no flow, we find roughly $c_1\approx 0.02$ from earlier shear-quench measurements [22]. We also set $Q_0=k_m$, where $k_m\simeq 1.2\times 10^4$ cm^{-1} along the flow direction at $t\approx 6$ s after shear quenching with $S\simeq 36$ s^{-1} [22]. The wave number k_m corresponds to the inverse of a characteristic size associated with the concentration domains during the phase-separation process and, hence, to the interfacial area per unit volume. We used a Runge-Kutta-Gill algorithm to solve the DO equations numerically, and the results obtained for $\Delta\eta/\eta^*$ are represented by the solid curve in Fig. 5. The DO theory predicts a much more rapid decay of the enhancement than has been measured. Furthermore, the theory attributes the decay to the decrease of the interfacial area Q. On the other hand, our observations of persistent streaks in the forward-scattered light has led us to conclude that, in fact, although $\Delta\eta/\eta^*$ decays, the interface does not, and remains in a highly anisotropic oriented stringlike form [16] that does not resist shearing.

We finally performed a set of experiments to investigate the shear-rate dependence of the viscosity of the phase-separating critical mixture as a function of the quench depth $T-T_c$. At a given value of the shear rate we raised the temperature of the mixture to the critical temperature, $T_c(P)$ being determined by the temperature where a spinodal ring appears in the absence of shear as registered by laser beam L_3 in Fig. 1, and then applied pressure quenches from $P_0+\Delta P$ to P_0 with ΔP varying from 0 to 1.96 bar in steps of 0.1 bar which corresponds to a resolution of 1 mK in temperature. These experiments were repeated for various values of the shear rate S in the range from 0.7 to 30 s^{-1}. The effective viscosity η, as determined from the first ten rotations of the inner cylinder after each quench, was fitted to a power law of the form

$$\eta\propto(S)^{-\omega_{\rm eff}}\ . \tag{4.8}$$

Our previous measurements of the viscosity as a function of the shear rate S in the homogeneous region had shown that at $T=T_c$ the viscosity does satisfy a power law with $\omega_{\rm eff}=0.021$, in accordance with Eq. (3.4). As discussed earlier, for quench depths $T-T_c<T_S-T_c$, the process of phase separation is suppressed and the dependence of the viscosity upon the shear rate is expected to remain the same. Indeed our earlier measurements have shown that the power law (4.8) is valid not only at $T=T_c$, but also $T=T_S>T_c$ [22]. However, for $T-T_c>T_S-T_c$, phase separation does take place and the viscosity will depend on time. Nevertheless, by averaging over the first ten cylinder rotations we were able to obtain an estimate of the S dependence of the effective viscosity during the time-dependent and highly nonlinear phenomenon of phase separation.

The values of the exponent $\omega_{\rm eff}$ thus obtained for the effective dependence of η on S are shown in Fig. 6 as a function of the quench depth $T-T_c$. For shallow quenches we again find $\omega_{\rm eff}(T)\simeq 0.02$, in accordance with Eq. (3.4), as is to be expected when $\delta_S\ge 1$. Somewhat larger values of $\omega_{\rm eff}(T)\simeq 0.03$ are observed for intermediate quench depths around $T-T_c\simeq 5$ mK, whereafter the value of $\omega_{\rm eff}(T)$ decreases as the quench depth is further increased. The most interesting feature of our results is that for large quench depths $T-T_c\simeq 20$ mK, the value of $\omega_{\rm eff}(T)$ falls to almost zero, even though for these large quench depths stringlike concentration domains are

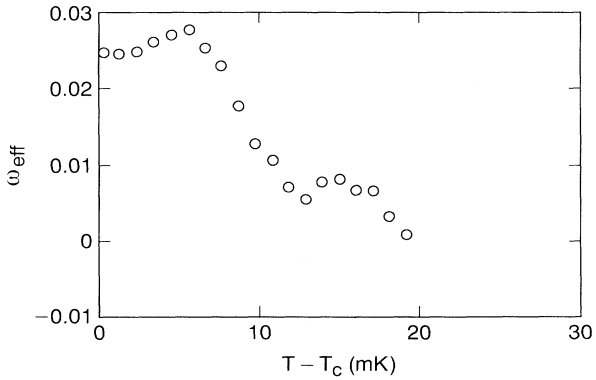

FIG. 6. The exponent $\omega_{\rm eff}(T)$ representing the effective S dependence of $\eta\propto(S)^{-\omega_{\rm eff}(T)}$ as a function of the quench depth $T-T_c$.

present as confirmed by the light-scattering patterns. This result indicates that even in the presence of elongated concentration domains the shearing stresses can be nearly proportional to the rate of shear, and the system effectively behaves as a Newtonian fluid again.

Our experiments suggest that the phase separation of a critical mixture under steady shear results in the formation of a stationary string phase in which the domains are stable and elongated but do not resist shearing. As we have noted, this behavior contradicts the current theories [5,17]. We conclude this section with some comments on observed rheological behaviors of phase-separating liquid mixtures that are in agreement with the theories, including those reported in our earlier papers. Onuki's theory [5] has been bound to describe off-critical mixtures. In this case isolated and compact concentration domains may grow by nucleation. Following the pioneering work by Taylor [46], Onuki argued that breakup of the domains in a shear flow should occur when they attain a size R such tht $\eta SR/\sigma \approx 0.3$. Recent experiments by Min and Goldburg have confirmed that this estimate is compatible with their observations of a phase-separating off-critical mixture [47]. Onuki also predicted for such systems a time-independent viscosity enhancement proportional to the volume fraction of the domains. In previous experiments we measured the viscosity of critical and off-critical phase-separating mixtures with an oscillating-disk viscometer [44,15]. For the off-critical mixtures, we found the behavior predicted by Onuki. In the case of the critical mixture, we found that the viscosity enhancement $\Delta\eta(t)=\eta(t)-\eta^*$ decreases to zero. Here again η^* is the viscosity free from the effects of domains. In this respect the behavior of the viscosity enhancement under oscillating shear is the same as the behavior reported in the present work for steady shear. However, the behavior found in the earlier work could be put into quantitative agreement with the theory for the critical system constructed by Doi and Ohta [17]. The reason is that, in the case where the shear rate S is oscillatory, Eqs. (4.4)–(4.6) allow for the behavior $\Delta\eta(t)/\eta^* \rightarrow 0$ with arbitrary values of the parameter μ. By treating this parameter as adjustable, we were able to fit our data. Again, the theory predicts that the interfacial area must decay to zero in order for the viscosity enhancement to do so. Without the light-scattering measurements that could test it, we accepted this prediction and interpreted it as indicating that oscillating shear is unable to stop the coalescence process of spinodal decomposition, so that a stationary state is never attained in this case. Possibly this interpretation is in fact correct; however, the more stringent test of the present experiment, which has combined rheological and scattering measurements, has shown that the theory is not adequate in general. Here, in experiments conducted under steady shear, we observe that the decay of the viscosity enhancement to zero occurs simultaneously with our observation of persistent, streaked, forward-scattered light. This scattering indicates that the interface attains a steady, flow-oriented stringlike state. We must conclude that this interfacial morphology has increased stability against coalescence and low resistance to shearing. This low resistance to shearing is at variance with the DO theory, which assumes that high interfacial anisotropy causes a large stress.

V. CONCLUSIONS

The present experiments have confirmed our previous observation [13] that at finite shear rates S the process of phase separation is suppressed until a characteristic temperature $T_S > T_c$ is reached corresponding to $St_{\xi'} \simeq 1$. Our experiments show that for $T > T_S$ a nearly stationary state is reached after quenching, accompanied by the formation of stringlike domains ordered in space along the flow direction, as found by Hasihimoto *et al.* [16] in polymer mixtures. Before attaining this stationary state the viscosity exhibits an enhancement, as suggested by recent theories, and whose magnitude depends on the shear rate S. However, this viscosity enhancement decays to zero as stable highly elongated concentration domains are formed, which, in contrast to recent theoretical predictions, do not appear to resist shearing. Such a string phase constitutes a dramatic illustration of unexpected shear-induced phenomena in phase-separating critical mixtures. We conclude that an improved theoretical treatment is required to obtain a full understanding of the structural changes and their rheological effects in phase-separating mixtures in the presence of shear.

ACKNOWLEDGMENTS

The authors are indebted to Y. Sugiyama and Y. Fukuda for valuable experimental assistance. In addition, the authors have benefited from discussions with A. Onuki, T. Ohta, M. Doi, F. Tanaka, H. Ushiki, and T. Yamamoto, who provided crucial contributions to the interpretation of our experiments. The research at Gunma University was supported by the Japanese Ministry of Education, Science and Culture under Grant No. 02640271, and the research at the University of Maryland by the National Science Foundation under Grant No. DMR-9215128.

[1] J. S. Huang, W. I. Goldburg, and A. W. Bjerkaas, Phys. Rev. Lett. **32**, 921 (1974).

[2] J. D. Gunton, M. San Miguel, and P. S. Sahni, in *Phase Transitions and Critical Phenomena,* edited by C. Domb and J. L. Lebowitz (Academic, New York, 1983), Vol. 8, p. 267.

[3] T. Hashimoto, in *Progress in Pacific Polymer Science,* edited by Y. Imanishi (Springer, Berlin, 1992), Vol. 2, p. 175.

[4] A. Onuki, Phys. Rev. A **34**, 3528 (1986).

[5] A. Onuki, Phys. Rev. A **35**, 5149 (1987).

[6] T. Ohta, H. Nozaki, and M. Doi, J. Chem. Phys. **93**, 2664 (1990).

[7] A. H. Krall, J. V. Sengers, and K. Hamano, Int. J. Thermophys. **10**, 309 (1989).

[8] A. Emanuele and M. B. Palma-Vittorelli, Phys. Rev. Lett. **69**, 81 (1992).

[9] P. C. Hohenberg and B. I. Halperin, Rev. Mod. Phys. **49**, 435 (1977).
[10] M. A. van Dijk, M. B. Eleveld, and A. van Veelen, Macromolecules **25**, 2274 (1992).
[11] T. Takebe, F. Fujioka, R. Sawaoka, and T. Hashimoto, J. Chem. Phys. **93**, 5271 (1990).
[12] T. Baumberger, F. Perrot, and D. Beysens, Physica A **174**, 31 (1991).
[13] K. Fukuhara, K. Hamano, N. Kuwahara, J. V. Sengers, and A. H. Krall, Phys. Lett. A **176**, 344 (1993).
[14] C. K. Chan and L. Lin, Europhys. Lett. **111**, 13 (1990).
[15] D. H. Rothman, Europhys. Lett. **14**, 337 (1991).
[16] T. Hashimoto, K. Matsuzaka, E. Moses, and A. Onuki (unpublished).
[17] M. Doi and T. Ohta, J. Chem. Phys. **95**, 1242 (1991).
[18] K. Hamano, N. Kuwahara, I. Mitsushima, K. Kubota, and J. Ito, Phys. Lett. A **150**, 405 (1990).
[19] K. Hamano, N. Kuwahara, I. Mitsushima, K. Kubota, and T. Kamura, J. Chem. Phys. **94**, 2172 (1991).
[20] K. Hamano, N. Kuwahara, K. Kubota, and I. Mitsushima, Phys. Rev. A **43**, 6881 (1991).
[21] N. Kuwahara, K. Hamano, and K. Kubota, Phys. Rev. A **44**, R6177 (1991).
[22] K. Hamano, S. Yamashita, and J. V. Sengers, Phys. Rev. Lett. **68**, 3579 (1992).
[23] J. C. Lang and R. D. Morgan, J. Chem. Phys. **73**, 5849 (1980).
[24] See, e.g., *Structure and Dynamics of Strongly Interacting Colloids and Supramolecular Aggregates in Solution,* edited by S.-H. Chen, J. S. Huang, and P. Tartaglia (Kluwer Academic, Dordrecht, 1992).
[25] B. H. Zimm and D. M. Crothers, Proc. Natl. Acad. Sci. USA **48**, 905 (1962).
[26] Y. Einaga, Y. Miyaki, and H. Fujita, J. Soc. Rheol. Jpn. **5**, 199 (1977).
[27] J. V. Sengers and J. T. R. Watson, J. Phys. Chem. Ref. Data **15**, 1291 (1986).
[28] N. C. Wong and C. M. Knobler, J. Chem. Phys. **69**, 725 (1970).
[29] N. C. Wong and C. M. Knobler, Phys. Rev. A **24**, 3205 (1981).
[30] F. Gonçalves, K. Hamano, and J. V. Sengers, Int. J. Thermophys. **10**, 845 (1989).
[31] E. A. Clerke and J. V. Sengers, Physica A **118**, 360 (1983).
[32] E. A. Clerke, J. V. Sengers, R. A. Ferrell, and J. K. Bhattacharjee, Phys. Rev. A **27**, 2140 (1983).
[33] A. Onuki, K. Yamazaki, and K. Kawasaki, Ann. Phys. (N.Y.) **131**, 217 (1981).
[34] D. Beysens, M. Gbadamassi, and B. Moncef-Bouanz, Phys. Rev. A **28**, 2491 (1983).
[35] K. Kawasaki, Ann. Phys. (N.Y.) **61**, 1 (1970).
[36] R. F. Berg and M. R. Moldover, J. Chem. Phys. **89**, 3694 (1988).
[37] J. C. Nieuwoudt and J. V. Sengers, J. Chem. Phys. **90**, 457 (1990).
[38] A. Onuki and K. Kawasaki, Phys. Lett. A **75**, 485 (1980).
[39] A. J. Liu and M. E. Fisher, Physica A **156**, 35 (1989).
[40] D. Beysens and F. Perrot, J. Phys. Lett. (Paris) **45**, L31 (1984).
[41] T. Takeba and T. Hashimoto, Polym. Commun. **29**, 261 (1988).
[42] D. Beysens, F. Perrot, and T. Baumberger, Physica A **204**, 76 (1994).
[43] E. D. Siggia, Phys. Rev. A **20**, 595 (1979).
[44] A. H. Krall, J. V. Sengers, and K. Hamano, Phys. Rev. Lett. **69**, 1963 (1992).
[45] A. H. Krall, J. V. Sengers, and K. Hamano, Phys. Rev. E **48**, 357 (1993).
[46] G. T. Taylor, Proc. R. Soc. London Ser. A **146**, 501 (1934).
[47] K. Y. Min and W. I. Goldburg, Phys. Rev. Lett. **71**, 569 (1993).

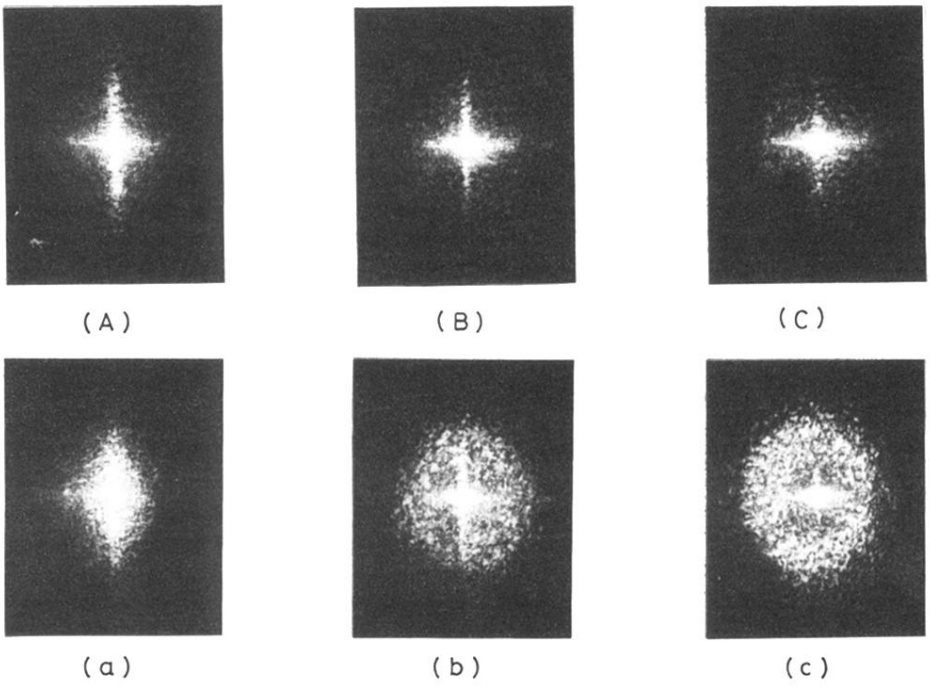

FIG. 3. Patterns of light scattered in the forward direction from the phase-separating critical mixture at $T \simeq T_c + 18$ mK after cessation of the shear from $S \simeq 0.8$ s^{-1} to 0 [(A) at $t \simeq 3$ s and (a) at $t \simeq 55$ s], from $S \simeq 7.6$ s^{-1} to 0 [(B) at $t \simeq 10$ s and (b) at $t \simeq 36$ s], and from $S \simeq 42$ s^{-1} to 0 [(C) at $t \simeq 3$ s and (c) at $t \simeq 35$ s].